

## Supporting Information

### Anchoring Boron Atom to the Specific Tetrahedral Sites of Borosilicate MFI by Imidazolium-based Molecules

**Authors:** Yufang Ma<sup>a</sup>, Lei Wang<sup>a\*</sup>, Lei Chen<sup>b</sup>, Meikun Shen<sup>c</sup>, Xue Yang<sup>d</sup>, Tengpeng Wang<sup>a</sup>, Feixiang Yuan<sup>a</sup>, Yu Zhou<sup>b</sup>, Jun Wang<sup>b</sup>, and Hongjun Zhu<sup>a\*</sup>

**Affiliations:**

<sup>a</sup>School of Chemistry and Molecular Engineering, Nanjing Tech University, Nanjing 211800, P. R. China

<sup>b</sup>State Key Laboratory of Materials-Oriented Chemical Engineering, College of Chemical Engineering, Nanjing Tech University, South Puzhu Rd. 30, Nanjing, 211816, P. R. China

<sup>c</sup>Department of Chemistry and Biochemistry, University of Oregon, 1585 E 13 Ave, Eugene, OR 97403, USA

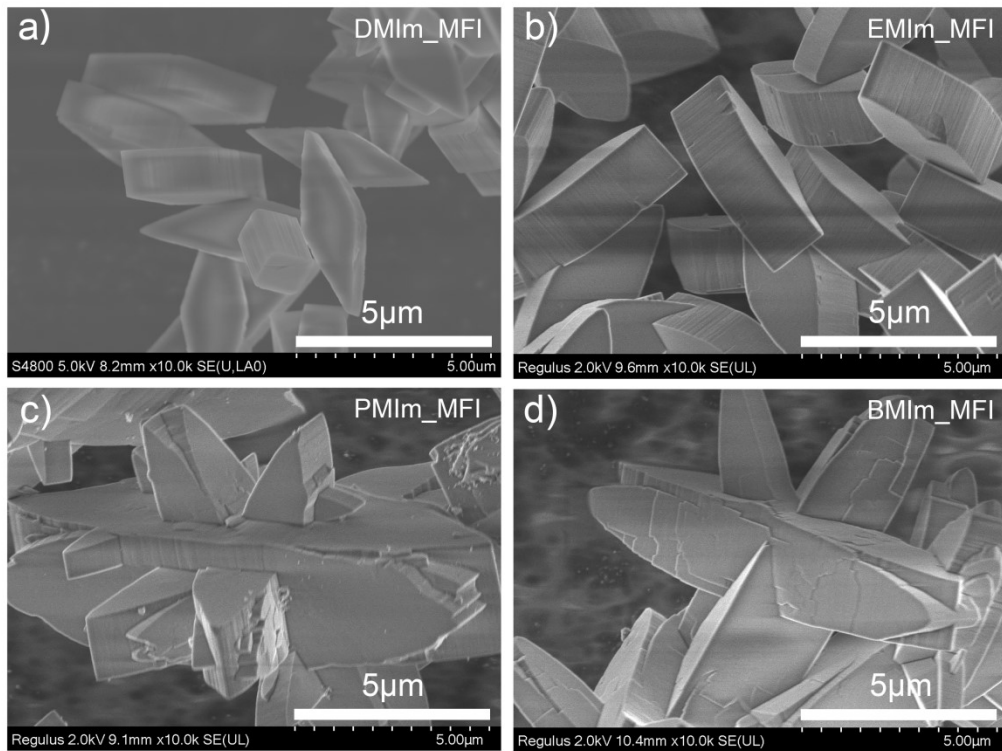
<sup>d</sup>Department of Chemistry, Shanghai Key Laboratory of Molecular Catalysis and Innovative Materials, Laboratory of Advanced Materials, and Collaborative Innovation Centre of Chemistry for Energy Materials, Fudan University, Handan Rd. 220, Shanghai, 200433, P. R. China

\*Corresponding Author:

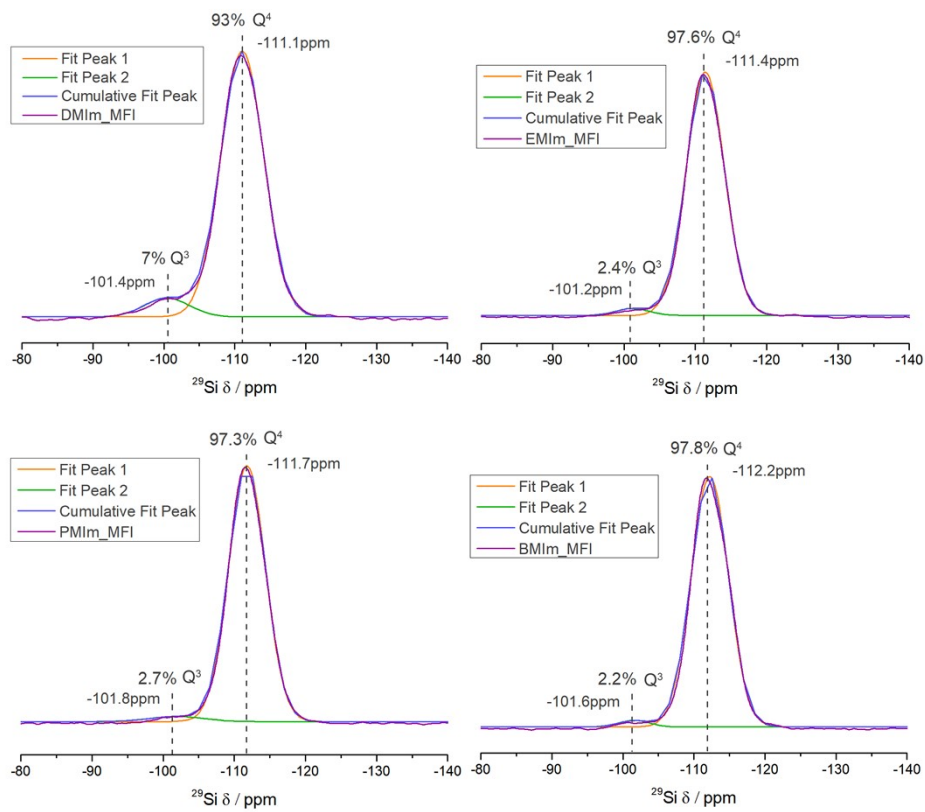
[L. Wang: l\\_wang19@njtech.edu.cn](mailto:l_wang19@njtech.edu.cn), [leiw.yz@outlook.com](mailto:leiw.yz@outlook.com), H. Zhu: [zhuhj@njtech.edu.cn](mailto:zhuhj@njtech.edu.cn)

## Table of contents

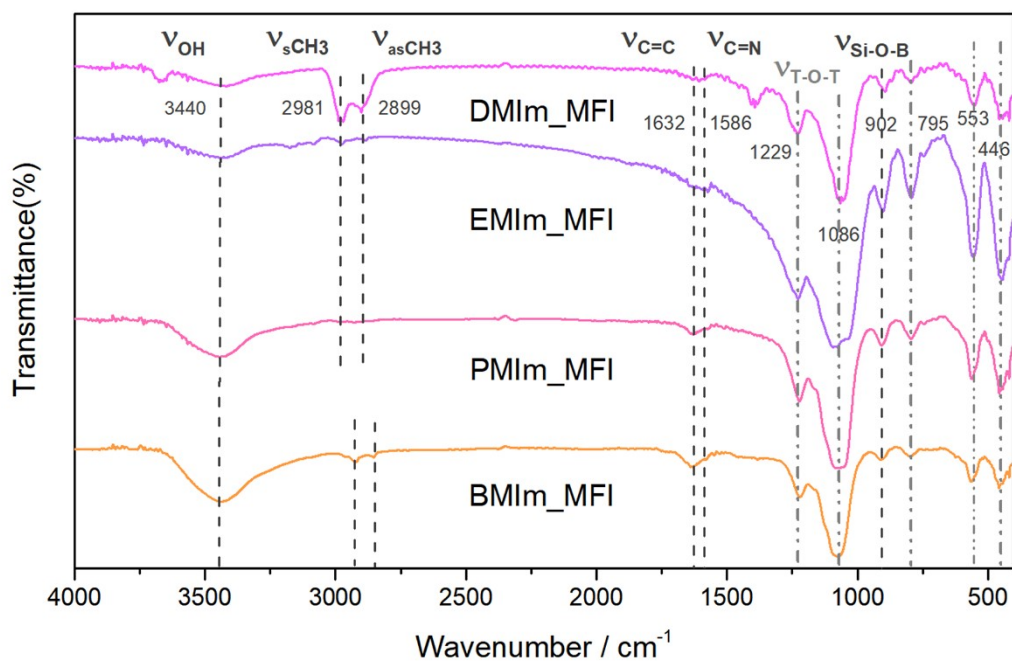
|  |    |
|--|----|
| <b>Figure S1.</b> Typical SEM images of as-synthesized borosilicate <b>MFI</b> zeolites. ....  | 3  |
| <b>Figure S2.</b> The relative quantity of Q <sup>3</sup> and Q <sup>4</sup> species in the as-synthesized borosilicate <b>MFI</b> zeolite.<br>.....   | 4  |
| <b>Figure S3.</b> FT-IR spectra of as-synthesized borosilicate <b>MFI</b> zeolites. ....   | 5  |
| <b>Figure S4.</b> Liquid <sup>13</sup> C (bottom: blue) NMR and solid-state <sup>1</sup> H→ <sup>13</sup> C CP/MAS NMR (top: black)<br>spectra of different borosilicate <b>MFI</b> synthesized using different OSDAs zeolites. ....   | 6  |
| <b>Figure S5.</b> TG-DTA-DSC profiles of as-synthesized borosilicate <b>MFI</b> zeolites. ....   | 7  |
| <b>Figure S6.</b> N <sub>2</sub> adsorption-desorption isotherms of calcined borosilicate <b>MFI</b> zeolites. ....  | 8  |
| <b>Figure S7.</b> Electron density map of as-synthesized borosilicate <b>MFI</b> zeolites. ....  | 9  |
| <b>Figure S8.</b> a) Rietveld refinement profiles of borosilicate <b>MFI</b> zeolite synthesized by TPA <sup>+</sup> cation,<br>b) Electron density map of TPA directed borosilicate <b>MFI</b> zeolite. c) Projection viewed along the<br>[100] direction, and d) the projection viewed along the [010] direction, respectively. .... | 10 |
| <b>Figure S9.</b> Rietveld refinement profiles of as-synthesized borosilicate <b>MFI</b> zeolites. ....  | 11 |
| <b>Figure S10.</b> The distribution of OSDAs in the as-synthesized borosilicate <b>MFI</b> framework. ....   | 12 |
| <b>Table S1.</b> Phase diagram of different OSDAs. ....  | 13 |
| <b>Table S2.</b> General composition of different borosilicate <b>MFI</b> zeolites. ....   | 14 |
| <b>Table S3.</b> Physical sorption details of calcined zeolites. ....  | 15 |
| <b>Table S4.</b> Rietveld refinement profiles of as-synthesized borosilicate <b>MFI</b> zeolites. ....   | 16 |
| <b>Table S5.</b> Boron enriched T sites in the reported borosilicates. ....  | 17 |



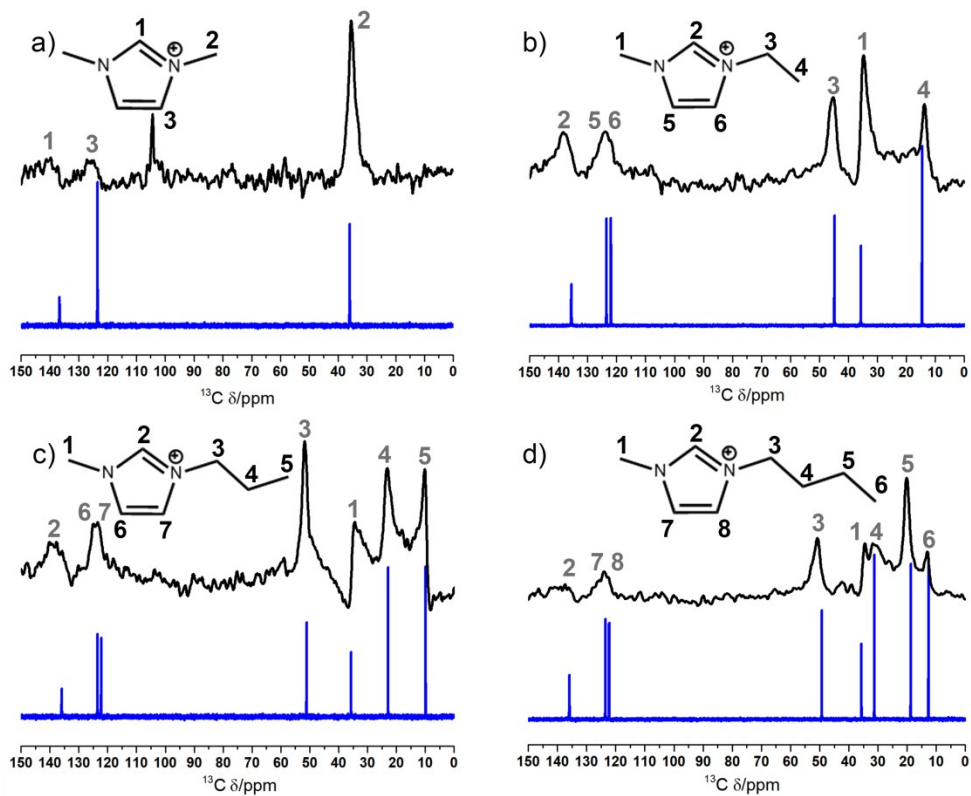
**Figure S1.** Typical SEM images of as-synthesized borosilicate **MFI** zeolites.



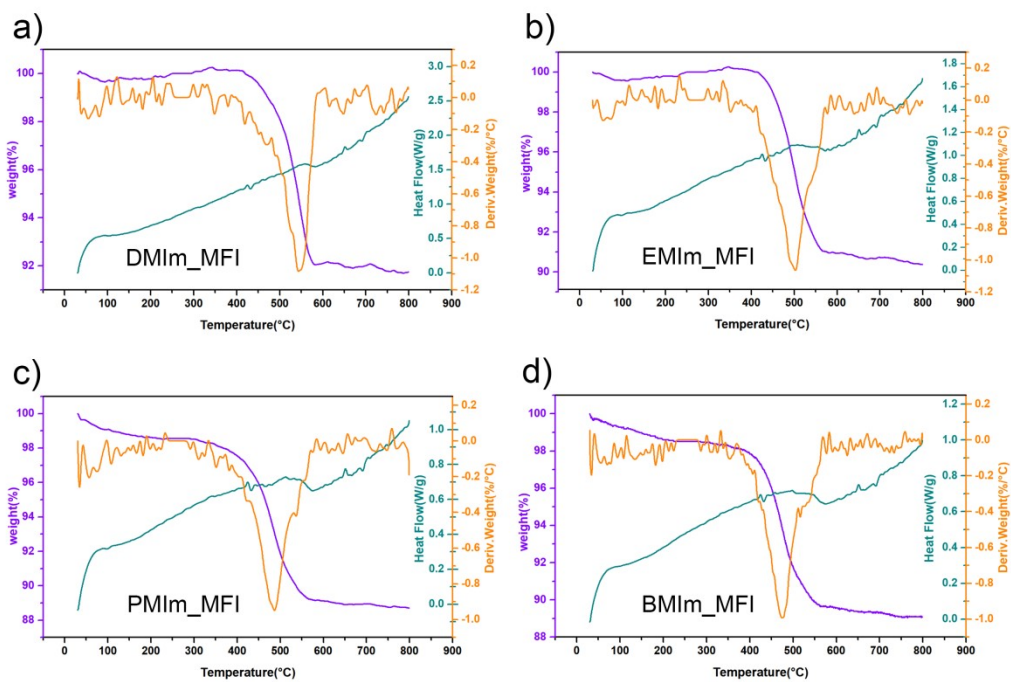
**Figure S2.** The relative quantity of Q<sup>3</sup> and Q<sup>4</sup> species in the as-synthesized borosilicate MFI zeolite.



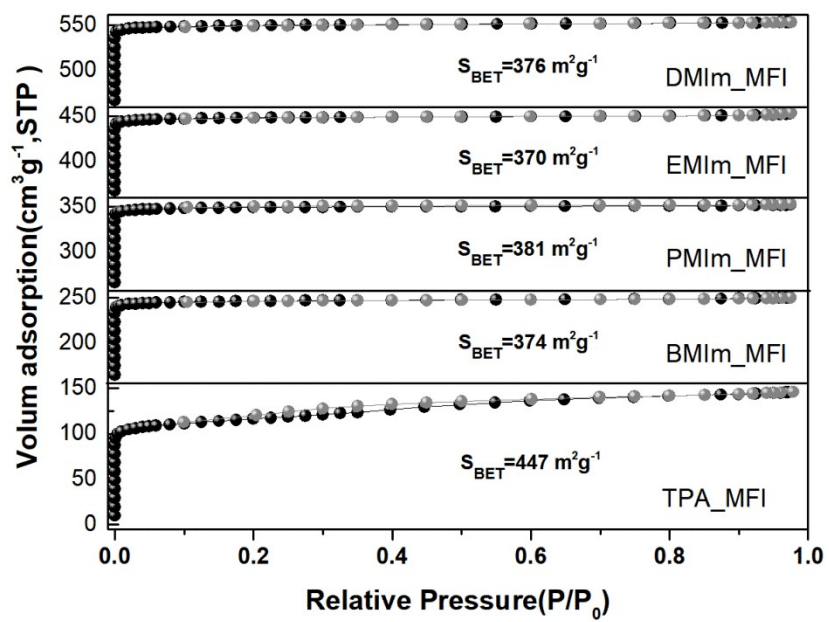
**Figure S3.** FT-IR spectra of as-synthesized borosilicate **MFI** zeolites.



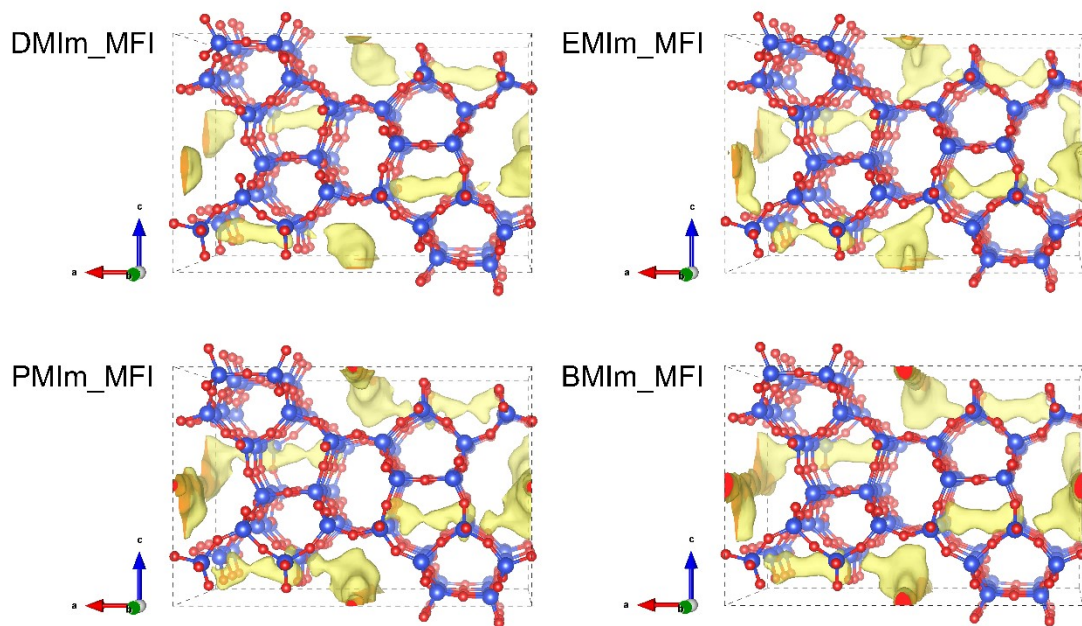
**Figure S4.** Liquid  $^{13}\text{C}$  (bottom: blue) NMR and solid-state  $^1\text{H}\rightarrow^{13}\text{C}$  CP/MAS NMR (top: black) spectra of different borosilicate **MFI** synthesized using different OSDAs zeolites.



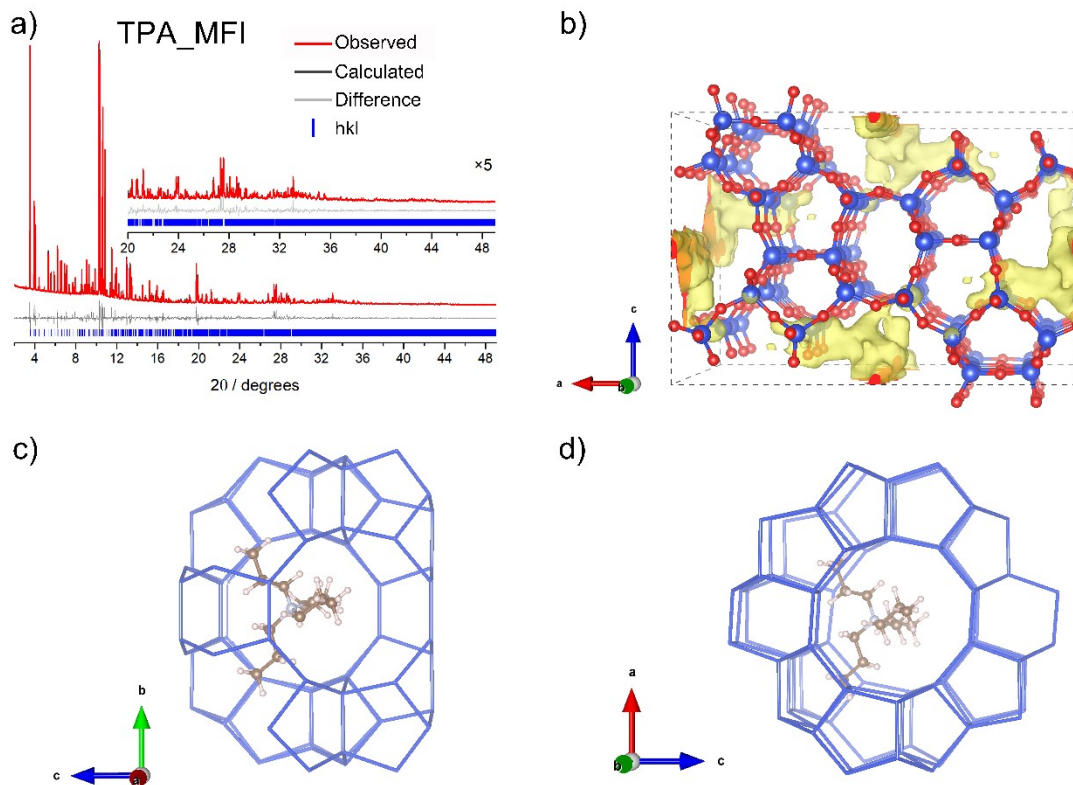
**Figure S5.** TG-DTA-DSC profiles of as-synthesized borosilicate **MFI** zeolites.



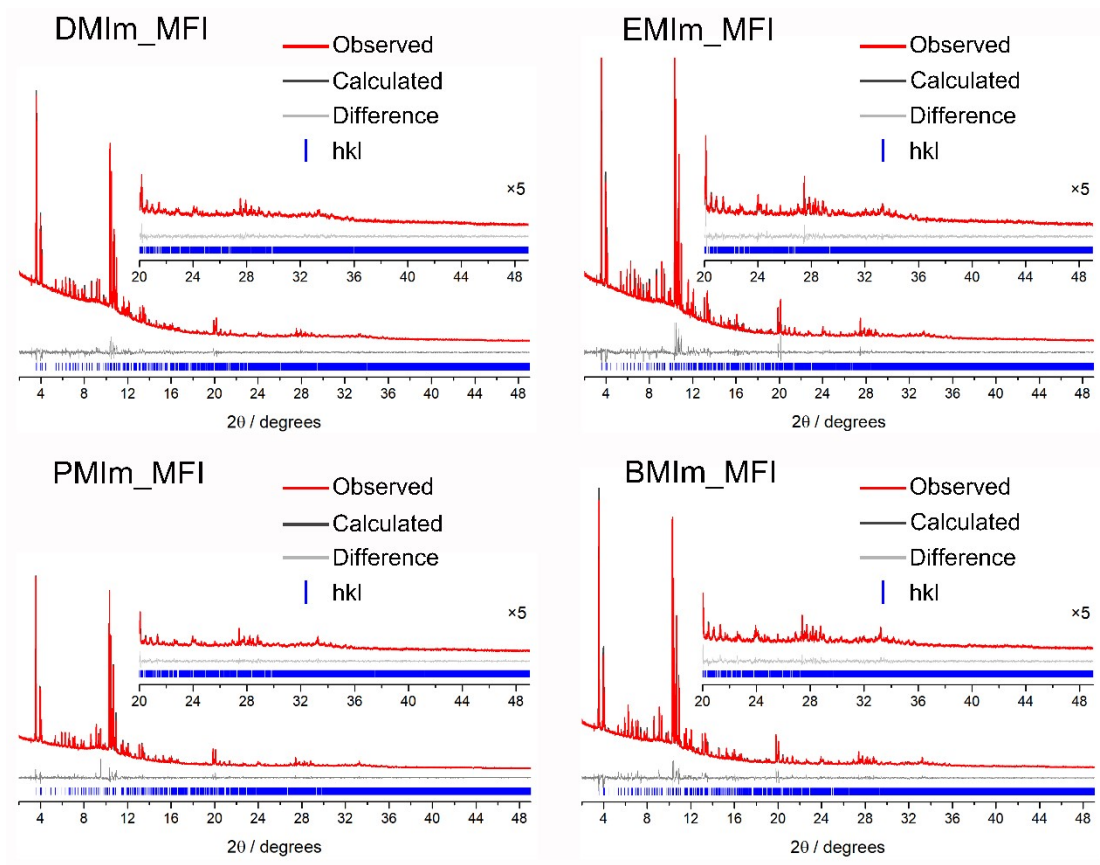
**Figure S6.** N<sub>2</sub> adsorption-desorption isotherms of calcined borosilicate **MFI** zeolites.



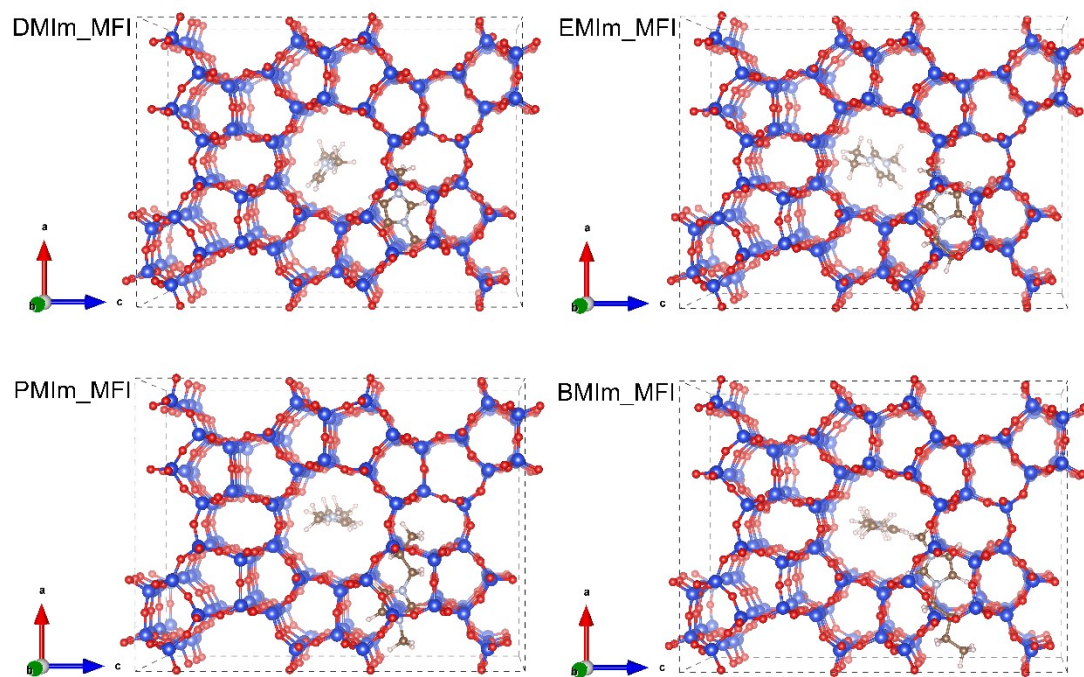
**Figure S7.** Electron density map of as-synthesized borosilicate **MFI** zeolites.



**Figure S8.** a) Rietveld refinement profiles of borosilicate **MFI** zeolite synthesized by TPA<sup>+</sup> cation, b) Electron density map of TPA directed borosilicate **MFI** zeolite. c) Projection viewed along the [100] direction, and d) the projection viewed along the [010] direction, respectively.

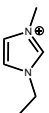
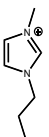
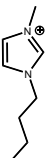


**Figure S9.** Rietveld refinement profiles of as-synthesized borosilicate **MFI** zeolites.



**Figure S10.** The distribution of OSDAs in the as-synthesized borosilicate **MFI** framework.

**Table S1.** Phase diagram of different OSDAs.

|   | OH/T<br>Si/B | 0.38       | 0.37       | 0.36       | 0.34       | 0.33       | 0.31       |
|---|--------------|------------|------------|------------|------------|------------|------------|
|    | 5            | TON+quartz | TON+quartz | TON+quartz | TON+quartz | TON+quartz | TON+quartz |
|   | 10           | TON+quartz | TON+quartz | TON+quartz | TON+quartz | TON+quartz | TON+quartz |
|   | 15           | TON        | TON        | MFI        | MFI        | Multiphase | Multiphase |
|   | 20           | TON        | TON+quartz | TON+quartz | TON+quartz | TON+quartz | TON+quartz |
|   | 25           | TON        | TON+quartz | TON        | TON        | TON+quartz | TON        |
|   | 50           | TON        | TON        | TON        | TON+quartz | TON+quartz | TON+quartz |
|    | 5            | TON+MFI    | TON+MFI    | TON+MFI    | TON+MFI    | TON        | MFI        |
|   | 10           | MFI+quartz | Multiphase | Multiphase | Multiphase | TON+MFI    | Multiphase |
|   | 15           | MFI        | TON+MFI    | MFI        | TON+MFI    | TON+MFI    | TON+MFI    |
|   | 20           | TON+quartz | TON+quartz | MFI+quartz | TON        | TON        | TON+quartz |
|   | 25           | TON+quartz | TON+quartz | TON+quartz | TON+quartz | TON+quartz | TON+quartz |
|   | 50           | TON        | TON+quartz | TON        | TON        | TON+quartz | TON        |
|   | 5            | MFI+TON    | MFI+quartz | MFI        | MFI+TON    | MFI+quartz | MFI        |
|   | 10           | MFI+TON    | MFI+quartz | MFI+quartz | MFI+quartz | MFI+quartz | MFI+quartz |
|   | 15           | TON+MFI    | MFI+TON    | MFI        | MFI+TON    | MFI+TON    | MFI+TON    |
|   | 20           | MFI        | MFI        | MFI        | MFI        | MFI        | MFI        |
|   | 25           | TON+quartz | TON+quartz | MFI+quartz | MFI+quartz | MFI+quartz | TON+quartz |
|   | 50           | MFI+quartz | MFI+quartz | MFI+quartz | TON+quartz | TON+quartz | MFI+quartz |
|  | 5            | MFI+ANA    | MFI+ANA    | MFI+ANA    | MFI+ANA    | MFI        | MFI+quartz |
|   | 10           | TON+MFI    | TON+MFI    | TON+MFI    | MFI        | MFI+TON    | MFI+quartz |
|   | 15           | MFI+quartz | MFI+quartz | MFI        | MFI+quartz | MFI+TON    | TON        |
|   | 20           | MFI+quartz | MFI+quartz | MFI+quartz | TON+quartz | TON+quartz | TON+quartz |
|   | 25           | TON+MFI    | Multiphase | MFI        | MFI        | MFI+TON    | TON+MFI    |
|   | 50           | TON+quartz | TON+quartz | TON+quartz | TON        | TON+quartz | TON        |

**Note:** The gel composition is 1 SiO<sub>2</sub> : x B<sub>2</sub>O<sub>3</sub> : y NaOH : 0.18 OSDA : 84 H<sub>2</sub>O (0.02≤x≤0.20; 0.31≤y≤0.38), where OSDA used: 1, 3-dimethylimidazole , 1-ethyl-3-methylimidazole , 1-propyl-3-methylimidazole, 1-butyl-3-methylimidazole , respectively.

**Table S2.** General composition of different borosilicate **MFI** zeolites.

| Entry           | General Composition   | Number of OSDA/u.c. | Compensate by OSDA | Si/B Ratio <sup>a</sup> |
|-----------------|---|---------------------|--------------------|-------------------------|
| <b>DMIm_MFI</b> | $[\text{Na}_{0.22}(\text{C}_5\text{H}_9\text{N}_2)_{5.58}][\text{B}_{6.29}\text{Si}_{89.71}\text{O}_{192}]$                               | 5.58                | 89%                | 14.26                   |
| <b>EMIm_MFI</b> | $[\text{Na}_{0.56}(\text{C}_6\text{H}_{11}\text{N}_2)_{4.39}(\text{H}_2\text{O})_{8.77}][\text{B}_{4.95}\text{Si}_{91.05}\text{O}_{192}]$ | 4.39                | 89%                | 18.39                   |
| <b>PMIm_MFI</b> | $[\text{Na}_{0.04}(\text{C}_7\text{H}_{13}\text{N}_2)_{6.25}(\text{H}_2\text{O})_{0.30}][\text{B}_{6.29}\text{Si}_{89.71}\text{O}_{192}]$ | 6.25                | 99%                | 14.26                   |
| <b>BMIm_MFI</b> | $[\text{Na}_{0.42}(\text{C}_8\text{H}_{15}\text{N}_2)_{4.06}(\text{H}_2\text{O})_{1.30}][\text{B}_{4.48}\text{Si}_{91.52}\text{O}_{192}]$ | 4.06                | 91%                | 20.42                   |

*Note:* <sup>a</sup> The Si/B ratio was determined by ICP results.

**Table S3.** Physical sorption details of calcined zeolites.

| Entry    | BET surface area <sup>a</sup> / m <sup>2</sup> g <sup>-1</sup> | Langmuir Surface area <sup>b</sup> / m <sup>2</sup> g <sup>-1</sup> | Single point surface area <sup>c</sup> at p/p <sub>0</sub> = 0.02/ m <sup>2</sup> g <sup>-1</sup> | Total pore volume <sup>d</sup> / cm <sup>3</sup> g <sup>-1</sup> | Micropore volume <sup>d</sup> /cm <sup>3</sup> g <sup>-1</sup> |
|----------|--|---|---|--|--|
| DMIm_MFI | 374  | 394   | 373   | 0.15   | 0.14   |
| EMIm_MFI | 381  | 399   | 380   | 0.15   | 0.14   |
| PMIm_MFI | 370  | 390   | 369   | 0.15   | 0.14   |
| BMIm_MFI | 376  | 396   | 376   | 0.15   | 0.14   |
| TPA_MFI  | 447  | 491   | 445   | 0.23   | 0.16   |

**Note:** <sup>a</sup>Calculated by the BET method; <sup>b</sup>Calculated by the Langmuir method; <sup>c</sup> Single point adsorption total pore volume of pores less than 79 nm width at p/p<sub>0</sub> = 0.98. <sup>d</sup> Calculated by the *t*-plot method.

**Table S4.** Rietveld refinement profiles of as-made borosilicate MFI zeolites.

|  | DMIm_MFI  | EMIm_MFI   | PMIm_MFI  | BMIm_MFI  | TPA_MFI   |
|--|---|--|---|---|---|
| <b>Crystal system</b>                          | orthorhombic  | orthorhombic   | orthorhombic  | orthorhombic  | orthorhombic  |
| <b>Space group</b>                             | <i>Pnma</i>   | <i>Pnma</i>  | <i>Pnma</i>   | <i>Pnma</i>   | <i>Pnma</i>   |
| <b>Chemical Formula</b>                        | $[\text{Na}_{0.22}(\text{C}_6\text{H}_9\text{N}_2)_{5.58}]$<br>$[\text{B}_{6.29}\text{Si}_{89.71}\text{O}_{192}]$ | $[\text{Na}_{0.56}(\text{C}_6\text{H}_{11}\text{N}_2)_{4.39}(\text{H}_2\text{O})_2]$<br>$[\text{B}_{.77}\text{Si}_{4.95}\text{O}_{91.05}]$ | $[\text{Na}_{0.04}(\text{C}_7\text{H}_{13}\text{N}_2)_{6.25}(\text{H}_2\text{O})_2]$<br>$[\text{B}_{0.30}\text{Si}_{6.29}\text{O}_{192}]$ | $[\text{Na}_{0.42}(\text{C}_8\text{H}_{15}\text{N}_2)_{4.06}(\text{H}_2\text{O})_1]$<br>$[\text{B}_{1.30}\text{Si}_{4.48}\text{O}_{91.52}]$ | $[\text{Na}_{2.34}(\text{C}_{12}\text{H}_{29}\text{NO})_{4.72}(\text{H}_2\text{O})_{0.68}]$<br>$[\text{B}_{0.7}\text{Si}_{93.7}\text{O}_{192}]$ |
| <b>Formula Weight</b>                          | 6042.36   | 6092.65  | 6475.63   | 6464.29   | 7277.65   |
| <b>OSDA/u.c.</b>                               | 5.58  | 4.39   | 6.25  | 4.06  | 4.72  |
| <b>2<math>\theta</math> range refinement/°</b> | 2-49  | 2-49   | 2-49  | 2-49  | 2-49  |
| <b>Refinement method</b>                       | Rietveld  | Rietveld   | Rietveld  | Rietveld  | Rietveld  |
| <b>Detector</b>                                | MYTHEN 1K   | MYTHEN 1K  | MYTHEN 1K   | MYTHEN 1K   | MYTHEN 1K   |
| <b>Sample holder</b>                           | spinning 0.5 mm<br>capillary  | spinning 0.5 mm<br>capillary   | spinning 0.5 mm capillary   | spinning 0.5 mm<br>capillary  | spinning 0.5 mm<br>capillary  |
| <b>Wavelength / Å</b>                          | 0.6887  | 0.6887   | 0.6887  | 0.6887  | 0.6887  |
| <b>2<math>\theta</math> Zero shift / °</b>     | -0.006441   | -0.002867  | -0.001228   | -0.003094   | -0.005006   |
| <b>Number of parameters</b>                    | 208   | 207  | 198   | 206   | 198   |
| <b>Number of <i>hkl</i>s</b>                   | 5017  | 5063   | 5102  | 5113  | 5198  |
| <b>a / Å</b>                                   | 19.9106(11)   | 19.9543(10)  | 19.9892(3)  | 19.9997(10)   | 20.0445(2)  |
| <b>b / Å</b>                                   | 19.6572(11)   | 19.7136(9)   | 19.7610(3)  | 19.7849(10)   | 19.9204(2)  |
| <b>c / Å</b>                                   | 13.2495(7)  | 13.2726(6)   | 13.3066(3)  | 13.3278(6)  | 13.3984(1)  |
| <b>V / Å<sup>3</sup></b>                       | 5185.7  | 5221.1   | 5256.20   | 5273.7  | 5349.89   |
| <b>Rwp/Rp/Rexp (%)</b>                         | 2.41 / 1.71 / 1.61  | 3.38 / 2.18 / 1.58   | 4.76 / 3.11 / 2.18  | 3.61 / 2.46 / 1.87  | 6.92 / 4.75 / 1.97  |
| <b>GoF</b>                                     | 1.49  | 2.14   | 2.01  | 1.92  | 3.51  |
| <b>CSD number</b>                              | 2119319   | 2119320  | 2119321   | 2119318   | 2121437   |

**Table S5.** Boron enriched T sites in the reported borosilicates.

| <b>Framework type code</b> | <b>Boron enriched T sites</b> | <b>Composite building units</b> |
|----------------------------|-------------------------------|---------------------------------|
| <b>MVY</b> (MCM-70)        | T4                            | 4-MR                            |
| <b>SEW</b> (SSZ-82)        | T10 T11                       | 4-MR                            |
| <b>EWS</b> (EMM-26)        | T4 T6 T7                      | 4-MR                            |
| <b>ATS</b> (SSZ-55)        | T1                            | 4-MR                            |
| <b>IFW</b> (SSZ-87)        | T7 T8                         | 4-MR                            |
| <b>SFN</b> (SSZ-59)        | T6 T7                         | 4-MR                            |